Development and Field Test of Modular Bridge Deck Made of GFRP Composite Materials

Jinwoo Jeong,*, Young-Ho Lee **, Kwang-Su Yeom **, Yoon-Kook Hwang**

* M. of Eng., Structural Engineering Dept, Korea Institute of Construction Technology, 2311 Daewha-Dong Ilsanseo-Gu Goyang, Gyeonggi-Do 411-712, Korea

** Dr. of Eng., Structural Engineering Dept, Korea Institute of Construction Technology, 2311 Daewha-Dong Ilsanseo-Gu Goyang, Gyeonggi-Do 411-712, Korea

A composite bridge deck system assembled from a modular profile with double-rectangular cell has been developed. This paper presents the developing process, install and field test of the GFRP decks, fabricated by a pultrusion process with E-glass fibers and vinyl ester resins. Numerical verification is performed by using general purpose finite element package ABAQUS. Design, manufacturing, installation, measure instrumentation, field test have been discussed in detail.

Key Words: Glass fiber reinforced Polymer (GFRP), Bridge deck, Pultrusion, Field test

1. Introduction

The fiber reinforced polymer composites are a state-of-the-art construction material, an alternative to traditional materials such as concrete, steel and wood. Specially, among many applications of FRP in civil infrastructures, bridge decks have received a great deal of attention because of their light weight, high strength-to-weight ratio, and corrosion resistance. Other advantages of FRP bridge decks are their reduction in bridge deck construction time and increase their service life. However, the FRP bridge decks also have disadvantages such as low modulus of elasticity translating into increased deflections, greater initial expense, and unfamiliarity to many engineers and constructors. Thus, further research, development and validation of the FRP deck systems are necessary in order to optimize and standardize these deck systems so that they are widely adopted in the industry. Currently, there are lack of comprehensive data based on the long-term response and need to provide cost-effective and efficient means of construction, non-destructive evaluation and health monitoring of these systems in the fields.

The FRP decks commercially available at present can be classified into two types: sandwich construction and adhesively bonded pultruded shape. The sandwich structure has been widely applied in the aerospace, marine, and automotive industries, where stiffness and strength requirements must be met with minimum weight. On the other hand, the adhesively bonded pultruded shape can be economically produced in continuous length using well-established methods such as a pultrusion process [1]. The modular construction of bridge deck systems enables quick project delivery.

Until now, there have been various theoretical and experimental studies to verify not only a technological and economical but also a numerical optimized solution at KICT [2, 3]. In this paper a composite bridge deck system assembled from modular profile with double-rectangular cell has been developed. The rectangular dual-cell profile is formed through a pultrusion process with E-glass fiber embedded in a vinyl ester resin. Installation and field test have been performed for GFRP deck consisting of multiple FRP box beams. Multi-cell box sections are commonly used in deck construction due to their efficient geometry and inherent stiffness in flexure and torsion. A numerical analysis by the finite element program ABAQUS has also been performed for verification. It should be noted that this project is still in progress and the results presented herein are preliminary.

2. Design & Manufacturing

2.1 Preliminary study

Based on the results of the preliminary study performed at KICT [1, 2], the standard design truckload DB-24 specified in the Specifications [4] with the tire contact area shown in Fig. 1

was assumed for a design live load. In addition, self-weight of the superstructure including the asphalt wearing surface was considered for the dead load. The overall design process was deflection limits since the flexural stiffness of GFRP is relatively low. The deflection limit of L/800 and the ultimate safety factor of five in the FHWA's advisory [5] were employed. Although the local buckling is not a failure mode, a safety factor of two was employed to ensure safety against buckling. Total height of the deck was limited to 200 mm so that the proposed deck can be used for the deck renewal projects. Using the proposed cross-sectional profiles, a GFRP deck prototype of a steel I-girder bridge was designed in the preliminary study. The single span bridge that is simply supported consists of a deck of 12.14 mm width and is supported by five 40 m-long steel girders spaced at 2.5 m.

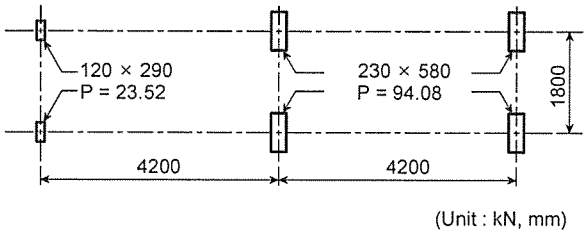

Fig. 1 DB-24 truck load and tire contact area

Designing the deck profile, a trapezoidal cross-sectional shape of the deck is identified as an optimum section for multi-cellular shapes. The structural performance of both the trapezoidal and rectangular sections is similar. However, if the proposed deck-to-girder connection is considered, the rectangular one may be more effective for the practical application.

The developed superstructure of the bridge is a pultruded material composed of E-glass fibers in various fiber orientations and a vinyl ester resin binder.

2.2 Fiber Architecture

The composite will generally have anisotropic properties unless randomly orientated fiber arrays are used in which case the composite will exhibit quasi-isotropic properties. The direction of the fiber such as unidirectional or bi-directional aligned or angle ply will determine the strength and stiffness of the composite. A typical pultruded section mainly includes the following three types of layer: (1) copped strand mats (CSMs) made of short fibers randomly oriented resulting in nearly isotropic in-plane properties, (2) multi-axial stitched fabrics and (3) rovings. Multi-axial stitched fabrics shown in Table 1 are a new reinforcement fabric with multi orientations combining the longitudinal (0°), transverse (90°), and double bias (±45°) directions, constructed with straight fibers and stitched together through the thickness direction to enhance interlamina properties of composites.

In this study, the fiber system of the decks was designed by DBT series, single-end rovings and chopped strand mats. The dimensions of unit module and fiber architectures are shown in Fig.2 and the thicknesses of top flange, bottom flange and web of the deck are 18, 16, and 11 mm respectively. It is noted that the thickness of the top flange is thicker than that of the bottom flange in consideration of the vehicle impact.

Table. 1 Layer construction

Fabric	Series	Stacking sequences	Series	Stacking sequences
Uniaxial	L	[0]	T	[90]
Biaxial & Double Bias	LT	[0/90]	DB	[45/-45]
Triaxial	DBL	[0/45/-45]	DBT	[45/90/-45]
Quadriaxial	DBLT	[0/45/90/-45]		

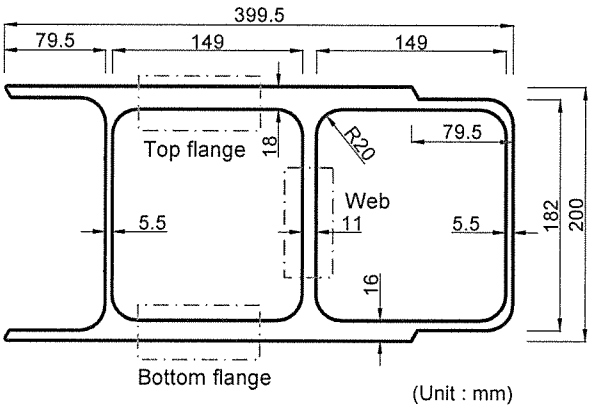

(a) Dimensions of unit module

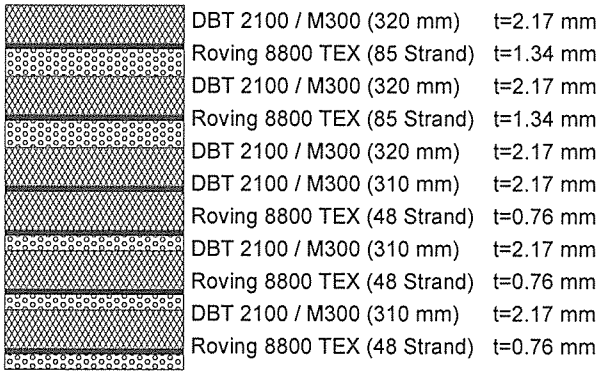

(b) Stacking sequences of the top flange

(c) Stacking sequences of the web

Fig. 2 Dimensions and stacking sequences of unit module

2.3 Material properties

Properties of many composite materials are strongly dependent on the arrangement and distribution of the fiber (fiber architecture). The constituent materials used for the GFRP deck consist of E-glass fibers and vinyl ester resin, and their properties are listed in Table. 2. Although most calculations on composite materials are based on the volume fractions of the constituents, it is sometimes important, particularly when calculating the density of the composite, to use weight fraction.

Table. 2 Properties of constituent materials.

Materials	E (GPa)	G (GPa)	υ	ρ (g/cm^3)
E-glass	72.5	27.6	0.22	2.54
Vynyl ester	3.4	1.2	0.38	1.12

In this study, it is assumed that the fiber weight fraction and resin weight fraction are 60 %, 40 %, respectively. The present approach is based on the elementary macromechanics. The fiber volume fraction can be calculated as follows:

$$V_f = \frac{\frac{w_f}{\rho_f}}{\frac{w_f}{\rho_f} + \frac{w_m}{\rho_m}}, \qquad V_m = 1 - V_f \tag{1}$$

where, V, w and ρ are volume fraction, weight and density, respectively.

The computation of lamina properties is an essential first step in the determination of the behavior of the component as a whole. Based on the fiber volume fraction, stiffness of each lamina shown in Table. 3 can be predicted from rules of mixture (ROM) of micromechanics model [6].

$$E_1 = E_f V_f + E_m V_m, \qquad E_2 = \frac{1}{\left(\frac{V_f}{E_f} + \frac{V_m}{E_m}\right)}$$
$$G_{12} = \frac{1}{\left(\frac{V_m}{G_m} + \frac{V_f}{G_f}\right)}, \qquad \nu_{12} = \nu_f V_f + \nu_m V_m \tag{2}$$

where, E_1, E_2 are Young's moduli along the fiber and perpendicular to fiber direction, G_{12} is shear ,moduli in 1-2 plane and ν_{12} is Poisson's ratio.

Table. 3 Lamina properties.

E_1 (Gpa)	30.83
E_2 (GPa)	5.48
G_{12} (GPa)	1.94
υ_{12}	0.32

Table. 4 Strength of constituent materials.

Components	Xt (MPa)	Yt (MPa)	Xc (MPa)	Yc (MPa)	S (MPa)
Flanges	335.3	84.1	177.3	89.9	64.2
Web	325.7	68.4	141.3	89.2	95.9

Table 4 provides the results of the coupon test. Xt and Xc indicate tensile and compressive strength in transverse direction shown in Fig. 5 respectively. Also, Yt and Yc are tensile and compressive strength in longitudinal (traffic) direction. S is in-plane shear strength.

2.4 Manufacturing

There are a number of techniques for manufacturing a polymer composite, all of which have an influence on the mechanical properties of the final composite. The pultrusion process involves pulling the glass fibers through a liquid resin bath and a set of heated dies to form the final geometric shapes (unit module) of the material, shown in Fig. 3. The finished pultrusion products can be variously geometrical cross-section shapes and generally straight. The pultrusion process is a continuous process. Therefore, the unit module must be cut to the proper length while the pultrusion process is carried out. Once several modules of the material have been fabricated, they are bonded together in the factory with an adhesive to form a deck. The length of these decks is typically equal to the width of the bridge.

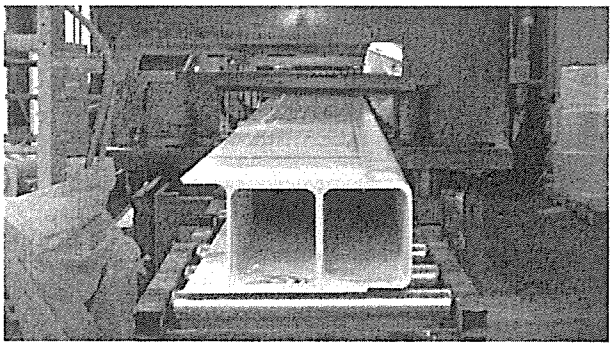

Fig. 3 Pultrusion process

3. Numerical Analysis

For numerical calculations, the general-purpose commercial finite element analysis program, ABAQUS [7], was used. The type of the finite element used in the analysis is an eight-node laminated shell element with reduced integration and six degrees of freedom per node (S8R). It is assumed that all parts of the deck system are perfectly bonded together.

One of the most demanding parameters during the finite element modeling of the structure is the material modeling. In this analysis, the direction of CSM is randomly distributed with

a short fiber, and assumed as quasi-isotropic. The fiber direction of the fabrics with DBT architecture is followed by the stacking sequence as given in Table 1. The rovings are assumed to be unidirectional fiber. The Tsai-Wu failure criterion [6] is used in order to predict failure load of the deck. The ABAQUS finite element model is shown in Fig. 4.

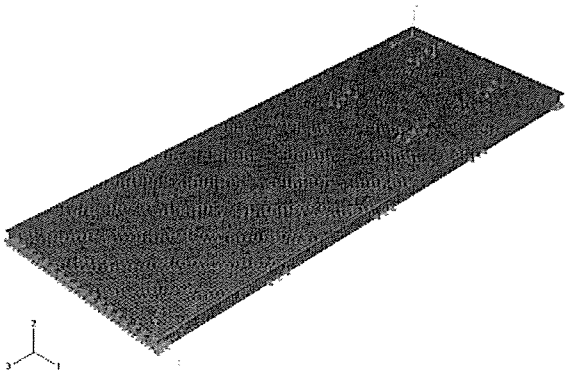

Fig. 4 ABAQUS FE-model

4. Field Testing

Although a number of demonstration projects have been completed worldwide [8-12], there is still a lack of information related to design criteria, cost and installation logistics and efficiency, and long-term response of the decks. In this study, the field test of the GFRP deck was performed to establish service load deflection, strain levels for future comparisons with field tests, to determine change in structural performance and long-term durability over time. An as-installed field evaluation through load test and further analytical investigations were considered essential to ensure the safe and cost-effective use of the FRP deck in future. The test details such as specimen, installation, instruments and evaluation are followed. All references to "longitudinal" and "transverse" are given with respect to the direction of traffic.

4.1 Specimen

The specimen is an assembly of nine of 8 m long unit module and 3 m wide, 200 mm deep with sand-blasting wearing surface of the top flange. Connection type used in the present study is adhesive over an 80 mm lap length. To stop slip of the deck in transverse direction, GFRP angles and elastic rubber pads as shown in Fig. 6 were attached under the bottom flange using adhesive.

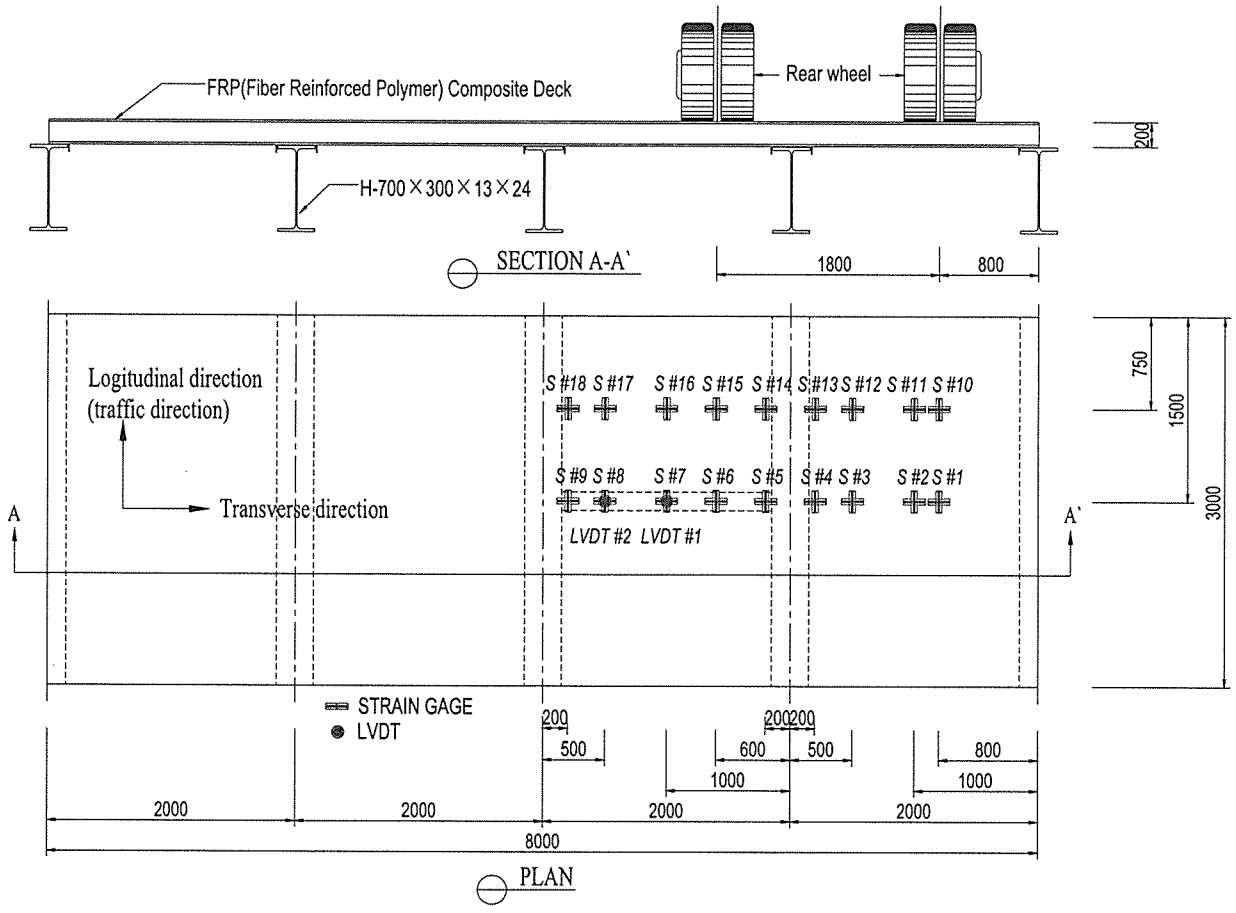

Fig. 5 Schematic of longitudinal positions for truck load and the locations of strain gages and LVDTs

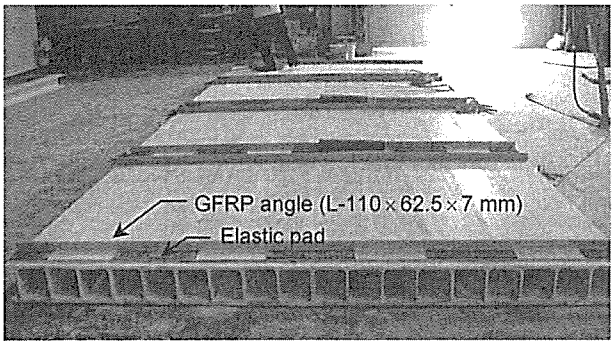

Fig. 6 Specimen

Fig. 8 Strain gages and LVDTs

4.2 Installation

For the field application and test, a subway construction site at Seoul was chosen. Generally, the steel deck and girder have been widely used for tentative construction and excavation work. In this site, the span of girder is regularly 2 m to install a standard steel deck, which is 2 m in length, 0.75 m in width, 0.2 m in height and 2.8 kN in weight per piece. After 16 pieces of temporary steel decks are removed, the GFRP deck is installed as shown in Fig. 7. With a total construction weight of 19.0 kN, installation was an easy task. Although the GFRP deck is designed to act compositely with the steel girders supporting them, the composite action between deck and girder was not considered in this application.

As a result, this deck system is very attractive as a replacement system since it may significantly reduce the dead load of the superstructure. Additionally, the deck is prefabricated and may be shipped and handled with relatively light equipment and minimal labor.

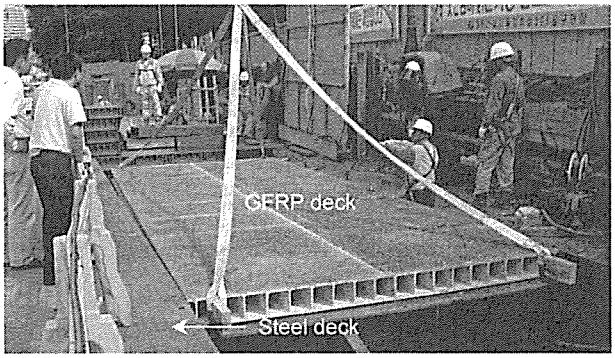

Fig. 7 Installation of GFRP deck

4.3 Instrumentation

The GFRP deck installed was a simply supported structure with no skew angle. The deck was instrumented with 36 strain gages mounted externally on the surface of the bottom flange. The locations of the strain gages are shown in Fig. 5. Gages at these locations were oriented in the both longitudinal and transverse directions. All the gages were made watertight and protected from the environment for long-term monitoring use. The linear variable differential transformers (LVDTs) as shown Fig. 7 were used to monitor the mid-span and quarter-span vertical deflections of the deck during the load test.

4.4 Evaluation

The truck load is determined by weighing each wheel set individually as shown in Table 5. The loading of the deck was accomplished with a dump truck placed at various locations. During each pass, the truck was stopped at seven longitudinal locations. Fig. 10 details the location of the truck stops. For the first load step, only the third axles of the truck were positioned on the GFRP deck from the longitudinal edge. In the second and third load steps, both of the second and third axles were positioned on the deck from the longitudinal edge and from the transverse centerline respectively. The forth load step positioned at the both second and third axles from the opposite edge of the load step 2. The truck was moved on and off from the deck and data was recorded at each step. This sequence was repeated 3 times to ensure the consistency of the recorded data. Due to the axle loads and axle spacing of the truck, the load step 2 corresponds to the worst loading condition.

Table. 5 Truck weights

	Front (P1) axles	Second (P2) axles	Third (P3) axles	Gross Weight
Weights (kN)	62.8	98.7	95.0	256.5

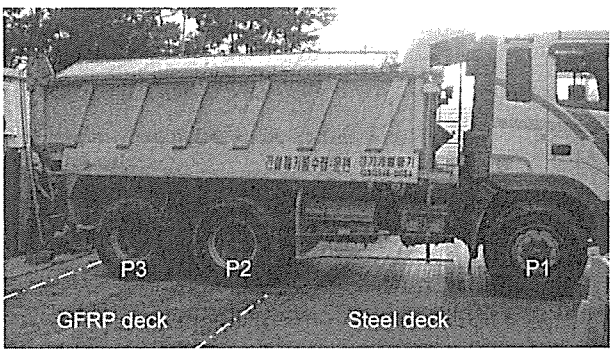

Fig. 9 Loading test of the GFRP deck

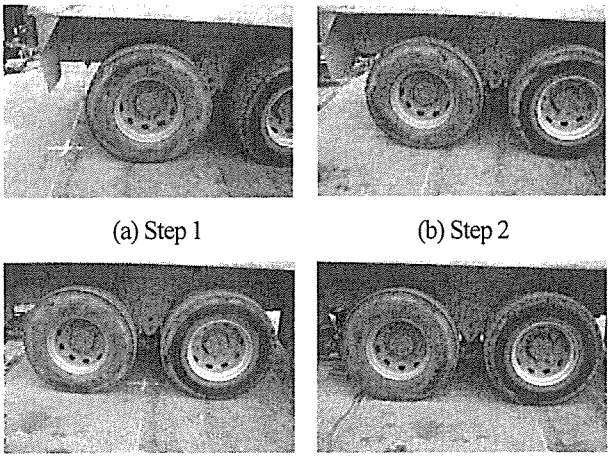

(a) Step 1 (b) Step 2

(c) Step 3 (d) Step 4

Fig. 10 Longitudinal truck locations

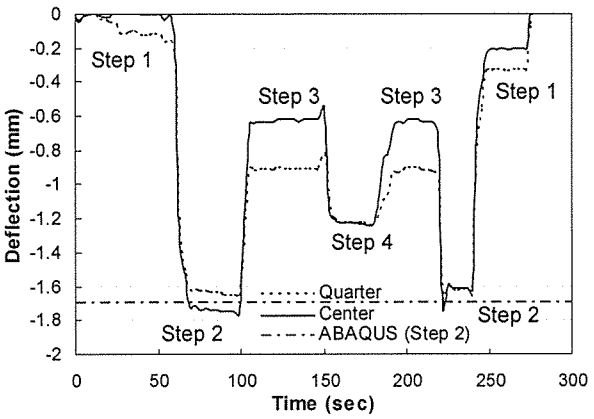

Fig. 11 Longitudinal truck locations

The results of the load test are presented in Fig. 11. The deflection of the center and quarter showed approximately 1.74 mm and 1.63 mm respectively. In comparison with the design target of L/800, in which the stiffness contribution from the pavement surface and barrier wall was not considered, the superstructure was significantly stiffer. The vertical deflection of the filed test results is compared with ABAQUS results in Fig. 11. The deflection of the deck matches with the ABAQUS results. The strains of longitudinal and transverse directions are shown in Fig. 12 at each step. The maximum strain was approximately 400 $\mu\varepsilon$, equivalent to 9 % of the ultimate strain capacity of the GFRP deck. The results show that the strain levels experienced in the deck are quite low but very high under the wheel loads. These local effects may play a major role in the performance of bridge components such as wearing surfaces, local buckling and shear lag and should be appropriately considered.

5. Conclusions

A composite bridge deck system assembled from a modular profile with double-rectangular cell has been developed for DB 24 load. Field test has been performed for cellular decks consisting of multiple GFRP box beams. A numerical analysis using the finite element program, ABAQUS, has also been performed for verification. It is found that the proposed GFRP deck meets deflection limit as well as strain limit, and is suitable for the bridge decks under DB24 load.

From the manufacturing, installation, field test and numerical verification of the present approach, the following remarks can be made:

• The manufacturing method has an influence of the accuracy of deck dimensions. Dimensional variations will make the installation more difficult and decrease the quality of field joints.

• For the design load test of the deck specimens, the deflection

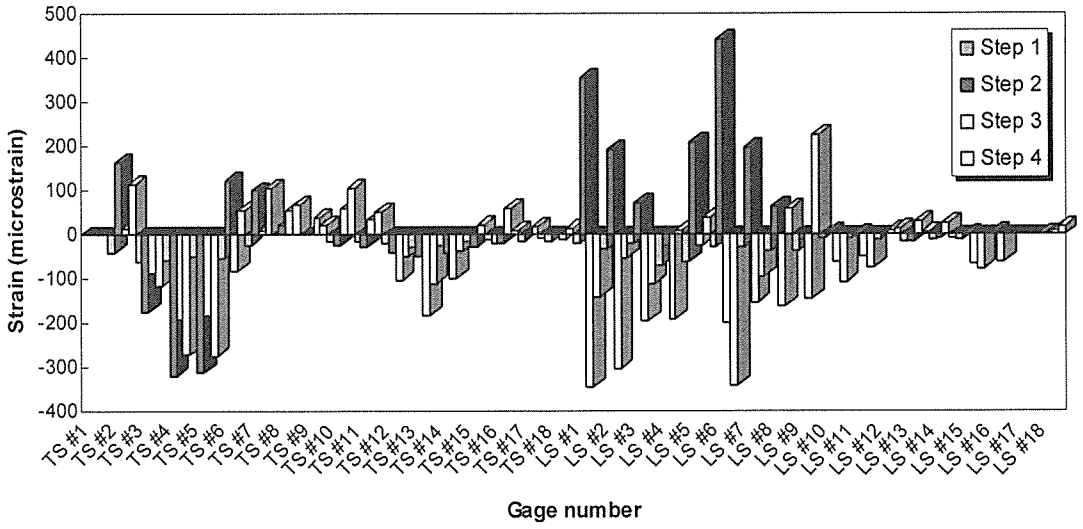

Fig. 12 Strains of longitudinal and transverse directions at each step

limit of the design specification is sufficiently satisfied and the maximum strains recoded were well below those predicted during design stages.

• A finite element model of the bridge has been developed and has been validated with previous and current study.

More experimental work such as static and dynamic test for rolling wheel loads on GFRP decks awaits further attention.

References

1) Bakis C.E, Bank L.C, Brown V.L, Cosenza E, Davalos J.F, Lesko J.J, et al., *Fibre-reinforced polymer composite for construction-state-of-art review*, ASCE, Journal of Composite for Construction, Vol. 6, No. 2, pp.73-87, 2002
2) H.Y. Kim, Y.K. Hwang, K.T. Park, Y.H Lee, S.M. Kim, *Fiber reinforced plastic deck profile for I-girder bridges*, Composite Structures, Vol. 67, No. 4, pp.411-416, 2005
3) K.T. Park, S.H. Kim, Y.H. Lee, Y.K. Hwang, *Pilot test on a developed GFRP bridge deck*, Composite Structures, Vol. 70, No. 1, pp.48-59, 2005
4) Ministry of Construction and Transportation (MOCT), *Standards specifications for highway bridges. 2nd edition*, Korea, 2000
5) American Association of State Highway and Transportation Official (AASHTO), *Standards specifications for highway bridges. 16th edition*, Washington, 1996
6) Jones R.M, *Mechanics of composite materials. 2nd edition*, Taylor & Francis, Inc., 1999
7) ABAQUS, *User's manual; version 6.5*, Hibbit, Karlesson & Sorensen, Inc., 2005
8) M.K. Turner, K.A. Harries, M.F. Petrou, D. Rizos, *In situ structural evaluation of a GFRP bridge system*, , Composite Structures, Vol. 65, No. 2, pp.157-165, 2004
9) A.J. Aref, S. Alampalli, Y. He, *Performance of a fiber reinforced polymer web core skew bridge superstructure. Part I: field testing and finite element simulations*, Composite Structures, Vol. 69, No. 4, pp.491-499, 2005
10) S. Alampalli, J. Kunin, *Rehabilitation and field testing of an FRP bridge deck on a truss bridge*, Composite Structures, Vol. 57, pp.273-375, 2002
11) D.C. Foster, D. Richards, B.R. Bogner, *Design and installation of fiber-reinforced polymer composite bridge*, ASCE, Vol. 4, No. 1, 2000
12) M. D. Hyers, J.J. Lesko, J. Haramis, T.E. Cousins, J. Gomez, P. Masarelli, *Laboratory and field testing of composite bridge superstructure*, ASCE, Vol. 4, No. 3, 2000